

# Journal of Materials Chemistry A

Accepted Manuscript



This is an *Accepted Manuscript*, which has been through the Royal Society of Chemistry peer review process and has been accepted for publication.

*Accepted Manuscripts* are published online shortly after acceptance, before technical editing, formatting and proof reading. Using this free service, authors can make their results available to the community, in citable form, before we publish the edited article. We will replace this *Accepted Manuscript* with the edited and formatted *Advance Article* as soon as it is available.

You can find more information about *Accepted Manuscripts* in the [Information for Authors](#).

Please note that technical editing may introduce minor changes to the text and/or graphics, which may alter content. The journal's standard [Terms & Conditions](#) and the [Ethical guidelines](#) still apply. In no event shall the Royal Society of Chemistry be held responsible for any errors or omissions in this *Accepted Manuscript* or any consequences arising from the use of any information it contains.

## Zwitterionic liquid crystals as 1D and 3D lithium ion transport media

zCite this: DOI: 10.1039/x0xx00000x

Bartolome Soberats,<sup>a,b</sup> Masafumi Yoshio,<sup>\*a</sup> Takahiro Ichikawa,<sup>c</sup> Hiroyuki Ohno<sup>c</sup> and Takashi Kato<sup>\*,a,b</sup>

Received 00th January 2012,

Accepted 00th January 2012

DOI: 10.1039/x0xx00000x

www.rsc.org/

We describe the development of self-assembled one- and three-dimensional lithium ion conductors composed of zwitterionic liquid crystals, lithium bis(trifluoromethylsulfonyl)imide (**LiTFSI**) and propylene carbonate (**PC**). Two types of wedge-shaped zwitterions based on imidazolium dicyanoethenolate and sulfonate were synthesized. These compounds alone show liquid-crystalline (LC) columnar hexagonal ( $\text{Col}_h$ ) phases and low ionic conductivities ( $10^{-8}$ - $10^{-7}$  S  $\text{cm}^{-1}$ ). The increase in the ionic conductivities was achieved by the addition of **LiTFSI** ( $10^{-5}$  S  $\text{cm}^{-1}$ ) followed by that of **PC** ( $10^{-4}$  S  $\text{cm}^{-1}$ ). Moreover, LC bicontinuous cubic ( $\text{Cub}_{\text{bi}}$ ) phases are induced by tuning the ionic nature of the zwitterionic liquid crystal with the ratio of **LiTFSI** and **PC**. The dissociation of **LiTFSI** in the zwitterions and the ion-dipole interaction between the lithium ion and **PC** are shown to be significant keys for the enhancement of the conductivities and stabilization of the nanosegregated LC structures.

### Introduction

Construction of supramolecular nanostructures with diverse functionalities using molecular self-assembly is of increasing interest for emerging nanotechnologies.<sup>1-19</sup> An important challenge is to build nanochannels capable of ion transport.<sup>21-44</sup> The use of liquid-crystalline (LC) self-assembly is a promising approach for the development of nanochannels with various dimensions and enhanced ion transport function.<sup>30-46</sup> Recently, LC ion-conductive materials has been applied to energy devices, such as lithium ion batteries and dye-sensitized solar cells.<sup>47-50</sup> Among the LC organizations, thermotropic LC bicontinuous cubic ( $\text{Cub}_{\text{bi}}$ ) assemblies attracted considerable attention because they form three-dimensionally interconnected ionic channels suitable for ion transport.<sup>34,38,44-46</sup> However, the design of three-dimensional (3D) ion-conductive thermotropic LC materials is still challenging because the formation of  $\text{Cub}_{\text{bi}}$  phases requires a delicate balance of volume and interactions between the polar and the non-polar parts in the material.<sup>44</sup> One of the approaches for induction of functional thermotropic  $\text{Cub}_{\text{bi}}$  phases is the use of two-component assemblies.<sup>51-54</sup> For example, we achieved 3D proton transport in the  $\text{Cub}_{\text{bi}}$  phases formed by complexation of zwitterionic molecules and organic acids.<sup>52,53</sup> The acid dissociates in the presence of zwitterions, which enables the proton transport. Interestingly, the proton conductivity and LC behavior are tuned by the amount of acid and also by the further addition of water.<sup>53</sup> LC  $\text{Cub}_{\text{bi}}$  phases were also induced for the complexes of a pyridinium-based zwitterions and lithium salts, although their ionic conductivities were not examined.<sup>54</sup> Anhydrous 3D lithium ion transport was previously achieved in LC materials by mixing lithium salts and ionic

molecules.<sup>31,55</sup> For example, we developed nanostructured polymer electrolytes upon photo-crosslinking of thermotropic LC  $\text{Cub}_{\text{bi}}$  assemblies composed of wedge-shaped ammonium salt and a lithium salt.<sup>55</sup> Gin and co-workers also reported LC  $\text{Cub}_{\text{bi}}$  polymer electrolytes based on the lyotropic LC assemblies of a polymerizable lithium sulfonate and a dilute  $\text{LiClO}_4$  solution in propylene carbonate (**PC**).<sup>31</sup> These approaches are based on the solubilization of lithium ions in nanostructured channels. However, we consider that the dissociation of lithium salts in zwitterionic LC media is a promising strategy for the development of lithium ion transport materials with induced  $\text{Cub}_{\text{bi}}$  phases.

Herein we report on the development of one-dimensional (1D) and 3D lithium ion transport channels (Fig. 1). We designed and prepared imidazolium-type zwitterions **1** and **2** (Fig. 2) to co-assemble with lithium bis(trifluoromethylsulfonyl)imide (**LiTFSI**) and **PC** forming well-defined ionic pathways capable of the lithium transport (Fig. 1 and Fig. 2). Our approach and material design in the present study is to use zwitterionic liquid crystals as media for the lithium ion transport. Zwitterionic liquid crystals tethering charge-delocalized anions are expected to form well-defined ionic channels, but have no transportable ions (Fig. 1, left). After addition of a lithium salt, the salt may be dissociated by the interactions with zwitterionic moieties, which allows lithium to move along the ionic pathways (Fig. 1 middle). At the same time, our intention is to increase the lithium ion mobility by the incorporation of **PC** as a polar additive (Fig. 1, right).<sup>31</sup> It is expected that the optimization of the ratio of additives, lithium salt and **PC**, can induce  $\text{Cub}_{\text{bi}}$  phases and enhance the ionic conductivities (Fig. 1).

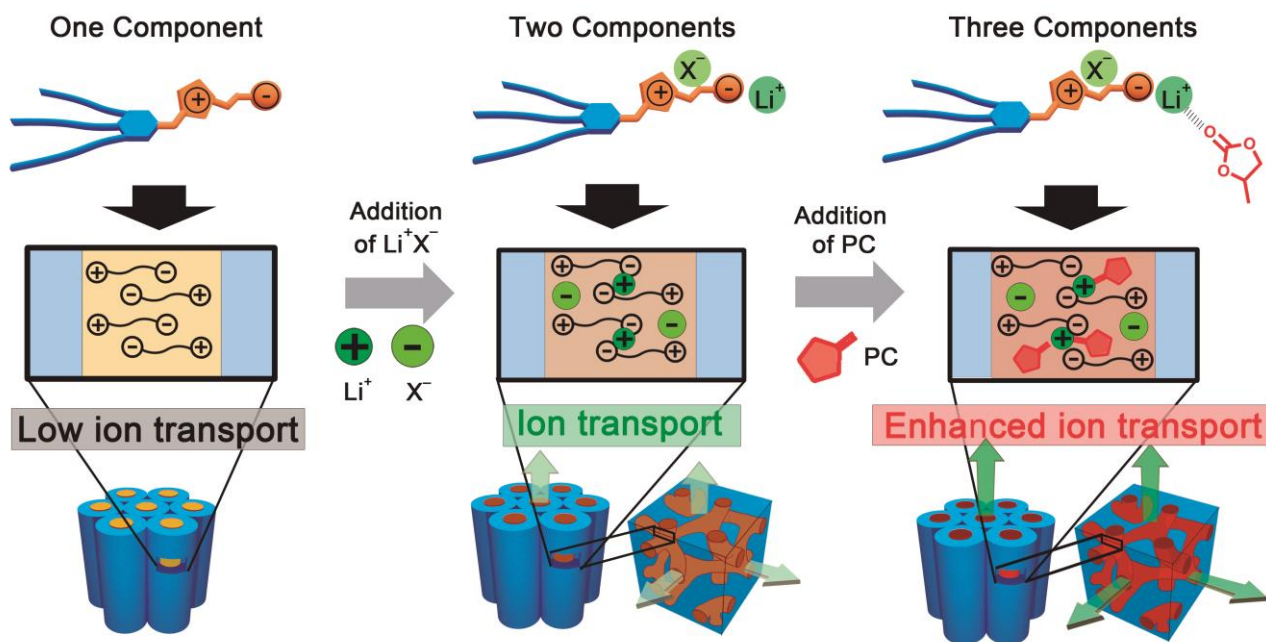


**Fig. 1** Our design strategy for the enhancement of lithium ion transport based on three components of nanostructured liquid-crystalline (LC) materials formed by the self-assembly of a zwitterionic liquid crystal, a lithium salt and propylene carbonate (PC). Green arrows indicate the direction of ion transport. The ionic channels are shown in yellow, orange, or red colors depending on their composition and the aliphatic parts are indicated in blue. The proposed organizations of molecules and salt inside the ionic channels are shown in the zoom windows from side views.

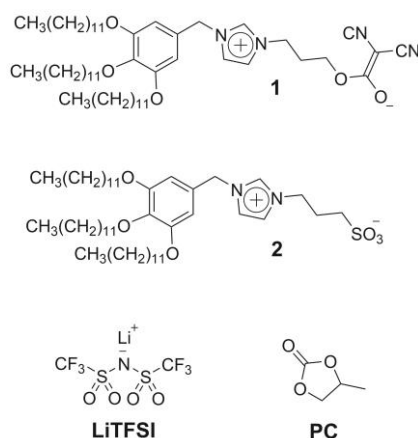


**Fig. 2** Chemical structures of the LC zwitterions **1** and **2**, lithium bis(trifluoromethylsulfonyl)imide (**LiTFSI**) and **PC**.

## Results and discussion

### Material design

Wedge-shaped zwitterions **1** and **2** (Fig. 2) are designed to act as LC ion transport media. The ionic parts of **1** and **2** consist of an imidazolium moiety tethering a dicyanoethenolate anion<sup>56-59</sup> or sulfonate anion<sup>52-54,60</sup> through a propylene spacer. We expected that compounds **1** and **2** would show different LC phase transition behavior and ion transport properties due to the differences in size of the anions and in the distribution of negative charges. **LiTFSI** (Fig.

2) is chosen as a lithium ion source because of its thermal stability and high delocalization of negative charge.<sup>35,54,61</sup> Ohno and co-workers previously reported that the equimolar mixtures of an imidazolium-based sulfobetaine whose melting point is over 100 °C and lithium salts (**LiTFSI**,  $\text{LiOSO}_2\text{CF}_3$ ,  $\text{LiBF}_4$ , and  $\text{LiClO}_4$ ) become room temperature ionic liquids.<sup>62</sup> Among them, the **LiTFSI** complex gives the lowest glass transition temperature and exhibits the highest ionic conductivity.<sup>62</sup> Lin and co-workers reported that the mixtures of imidazolium-type carboxylates or sulfonates and **LiTFSI** form smectic A phases exhibiting ionic conductivities.<sup>63,64</sup> In addition, the employment of bulky **LiTFSI** as an additive for zwitterionic liquid crystals, can induce the structural change of LC phases because of the change of the molecular shapes and volume balance between the polar and nonpolar parts.<sup>35,54</sup> Thus we considered that the complexation of **1** or **2** and **LiTFSI** would lead to the development of 3D lithium ion conductive materials exhibiting  $\text{Cub}_{\text{bi}}$  LC phases. Furthermore, to enhance the dissociation of lithium ion in the zwitterionic ion transport media, **PC** (Fig. 2) is used as a polar additive because the carbonyl group of **PC** has the ability to coordinate to lithium ions.<sup>31,40,48,61</sup>

### Supramolecular interactions between components

In order to examine the interactions between lithium ion, zwitterion and **PC**,  $^7\text{Li}$  NMR measurements of **LiTFSI**, the mixture of **1** and **LiTFSI** and tertiary mixture of **LiTFSI**, **1** and **PC** were conducted in the  $\text{CDCl}_3/\text{THF-}d_6$  solutions using  $\text{LiCl}$  in  $\text{D}_2\text{O}$  as an internal standard (Fig. 3). The results for **2** are shown in the ESI† (Fig. S10). The  $^7\text{Li}$  chemical shift of **LiTFSI** shows a downfield shift of 0.06 ppm in the presence of **1** (Fig. 3, middle). This result suggests the formation of a complex between **1** and **LiTFSI**, where the lithium ion may interact with the dicyanoethenolate anion (Fig. 1 top middle and Fig. S9).<sup>65,66</sup> The addition of **PC** to the mixture of **1** and **LiTFSI** induces a further downfield shift of 0.03 ppm (Fig. 3,

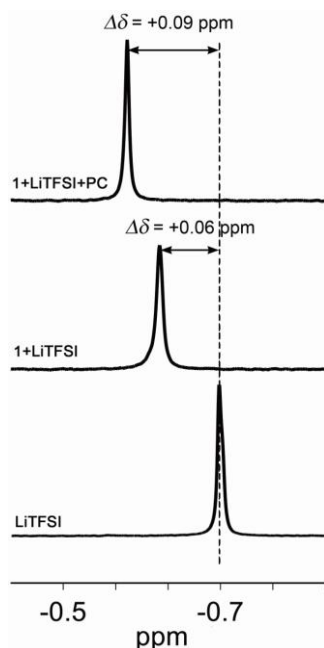


**Fig. 3**  $^7\text{Li}$  NMR spectra of **LiTFSI** (0.013 M, 450  $\mu\text{L}$ ) (bottom), **1/LiTFSI** (0.02 M/0.013 M, 450  $\mu\text{L}$ ) (middle) and **1/LiTFSI/PC** (0.02 M/0.013 M/0.13 M, 450  $\mu\text{L}$ ) (top) in  $\text{CDCl}_3\text{:THF-}d_6$  (v:v, 6:1) solution.  $\text{LiCl D}_2\text{O}$  solution in a coaxial NMR tube was used as an internal standard and the lithium signal was settled at 0 ppm. Dashed line indicates the chemical shift of the lithium ion for the pure **LiTFSI** solution. All the spectra were recorded at room temperature.

top) compared to the chemical shift for the mixture of **1** and **LiTFSI** (Fig. 3, middle). This shift may be attributed to the ion-dipole interactions between lithium ions and **PC**. It should be mentioned that the stepwise downfield shifts of  $^7\text{Li}$  signal are detected by the addition of zwitterions followed by **PC**, in spite of the presence of THF which is a competitive solvent.

The interactions between **1**, **LiTFSI** and **PC** were also confirmed by IR measurements in the bulk state. The IR spectra of **1**, the mixture of **1** and **LiTFSI** and tertiary mixture of **1**, **LiTFSI** and **PC** were recorded at room temperature (Fig. S11). Single compound **1** shows two absorption bands at 2193 and 2165  $\text{cm}^{-1}$  which are characteristic of the  $\text{C}\equiv\text{N}$  vibrations of the dicyanoethenolate moiety.<sup>57</sup> These bands are shifted to 2202 and 2173  $\text{cm}^{-1}$ , respectively, after the addition of 50 mol% of **LiTFSI**. Further addition of 10 wt% of **PC** resulted in the high wavenumber shift of CN bands to 2206 and 2179  $\text{cm}^{-1}$ , respectively. These results suggest the existence of interactions between zwitterionic molecule, **LiTFSI** and **PC**.

### Liquid-crystalline properties

Compounds **1** and **2** show LC columnar hexagonal ( $\text{Col}_h$ ) phases from room temperature to around 200  $^\circ\text{C}$  at which decomposition occurs (Table 1 and Table S1). Mixtures of the zwitterions with **LiTFSI** [**1/Li** $^+(x)$  and **2/Li** $^+(x)$ ,  $x$  denotes the mol% of **LiTFSI**] were prepared by mixing the THF solutions of **LiTFSI** and the zwitterions, followed by the evaporation of the solvent to yield the anhydrous mixtures as white solids. The liquid crystallinity of the **1/Li** $^+(x)$  and **2/Li** $^+(x)$  mixtures was examined by a polarizing optical microscope (POM), X-ray diffraction (XRD) and differential scanning calorimetry. The mixtures **1/Li** $^+(x)$  with 10–40 mol% of **LiTFSI** and all the mixtures **2/Li** $^+(x)$  exhibit only  $\text{Col}_h$  phases (Table 1 and Table

S1).<sup>†</sup> As for **1/Li** $^+(50)$ , the  $\text{Cub}_{\text{bi}}$  phase is induced in addition to the formation of  $\text{Col}_h$  phase. The  $\text{Cub}_{\text{bi}}$  phase is observed from room temperature to 65  $^\circ\text{C}$  and slowly changed to the  $\text{Col}_h$  phase between 65 and 88  $^\circ\text{C}$  under POM observation on the heating rate of 5  $^\circ\text{C min}^{-1}$ . The formation of ionic pairs composed of ionic liquid-like imidazolium TFSI and lithium dicyanoethenolate, which is bulkier than lithium sulfonate, may disturb the columnar packing.<sup>59</sup> The change in the volume fraction of the polar and nonpolar parts may also contribute to the induction of the  $\text{Cub}_{\text{bi}}$  phase.<sup>51–54</sup> Figures 4 and 5 show the XRD patterns and POM images of **1/Li** $^+(50)$  in the  $\text{Cub}_{\text{bi}}$  and  $\text{Col}_h$  phases. The small-angle XRD pattern of **1/Li** $^+(50)$  at 55  $^\circ\text{C}$  (Fig. 4a) shows two strong and three weak peaks at 39.2, 34.0, 25.7, 21.4 and 20.4  $\text{\AA}$  corresponding to the (211), (220), (321), (420) and (332) reflections, respectively. The reciprocal  $d$ -spacing ratio of these peaks is  $\sqrt{6}:\sqrt{8}:\sqrt{14}:\sqrt{20}:\sqrt{22}$ , which corresponds to a  $\text{Cub}_{\text{bi}}$  phase with an  $Ia3d$  symmetry. In contrast, the wide-angle XRD pattern of **1/Li** $^+(50)$  at 120  $^\circ\text{C}$  (Fig. 4b) shows the (100), (110) and (200) reflections, which are characteristic of a  $\text{Col}_h$  phase. The POM image of **1/Li** $^+(50)$  at 58  $^\circ\text{C}$  shows no birefringence (Fig. 5a), indicating the formation of a  $\text{Cub}_{\text{bi}}$  phase. On heating the sample to 90  $^\circ\text{C}$  (Fig. 5b), a birefringence upon the formation of the  $\text{Col}_h$  phase with polydomain organization is observed.

**Table 1** LC behavior of zwitterionic compounds and their mixtures with **LiTFSI** and/or **PC**.

Sample <sup>a</sup>	Phase transition behavior <sup>b</sup>			
<b>1</b>		$\text{Col}_h$	217	Decomp.
<b>1/Li</b> $^+(20)$		$\text{Col}_h$	190	Decomp.
<b>1/Li</b> $^+(50)$	$\text{Cub}_{\text{bi}}$	65–88	$\text{Col}_h$	190
<b>1/Li</b> $^+(20)\text{PC}(5)$	$\text{Cub}_{\text{bi}}$	50–68	$\text{Col}_h$	120 <sup>c</sup>
<b>1/Li</b> $^+(20)\text{PC}(10)$	$\text{Cub}_{\text{bi}}$	50–75	$\text{Col}_h$	120 <sup>c</sup>
<b>1/Li</b> $^+(50)\text{PC}(5)$	$\text{Cub}_{\text{bi}}$	81–92		Iso
<b>1/Li</b> $^+(50)\text{PC}(10)$	$\text{Cub}_{\text{bi}}$	74–86		Iso
<b>2</b>		$\text{Col}_h$	207	Decomp.
<b>2/Li</b> $^+(20)$		$\text{Col}_h$	200	Decomp.
<b>2/Li</b> $^+(50)$		$\text{Col}_h$	200	Decomp.
<b>2/Li</b> $^+(20)\text{PC}(5)$		$\text{Col}_h$	120 <sup>c</sup>	
<b>2/Li</b> $^+(20)\text{PC}(10)$		$\text{Col}_h$	120 <sup>c</sup>	
<b>2/Li</b> $^+(50)\text{PC}(5)$		$\text{Col}_h$	120 <sup>c</sup>	
<b>2/Li</b> $^+(50)\text{PC}(10)$		$\text{Col}_h$	120 <sup>c</sup>	

<sup>a</sup> Ratio of **LiTFSI** and **PC** is indicated as follows: **1/Li** $^+(x)$ , **2/Li** $^+(x)$ , **1/Li** $^+(x)\text{PC}(y)$  and **2/Li** $^+(x)\text{PC}(y)$ , where  $x$  is the mol% of **LiTFSI** and  $y$  indicates the wt% of **PC**. <sup>b</sup> Determined by polarizing optical microscope observation. The LC behavior was examined on heating processes (5  $^\circ\text{C min}^{-1}$ ) from 25  $^\circ\text{C}$  to decomposition or isotropization temperature of the sample. The given transition temperatures correspond to the starting of the phase transitions. In the case of slow phase transition, a temperature range is given. Mixtures containing more than 50 mol% of **LiTFSI** show no homogeneous LC phases. Mixtures with 15 wt% or more of **PC** showed biphasic behavior. <sup>c</sup> For **PC** containing samples, the microscopic observation was conducted up to 120  $^\circ\text{C}$ . All the mixtures showed decomposition at around 200  $^\circ\text{C}$ .  $\text{Col}_h$ : columnar hexagonal,  $\text{Cub}_{\text{bi}}$ : bicontinuous cubic, Iso: isotropic, Decomp.: decomposition

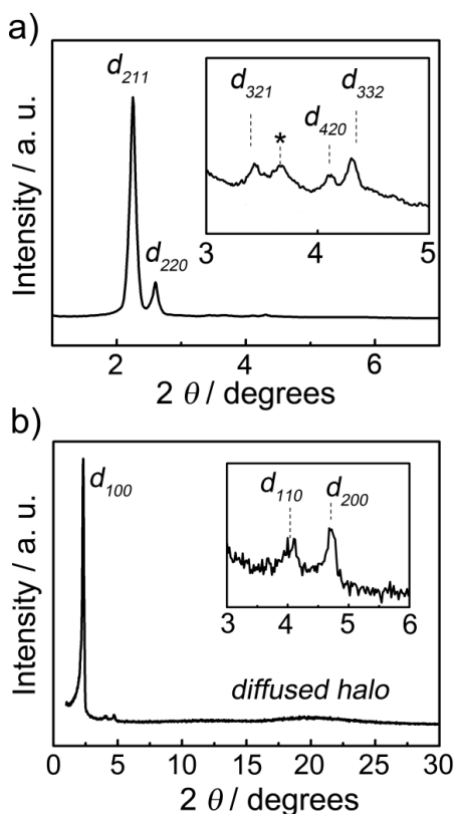


**Fig. 4** X-ray diffraction (XRD) patterns of **1/Li<sup>+</sup>(50)** at a) 55 °C and b) 120 °C. The mark \* corresponds to the diffraction of the Kapton® film.

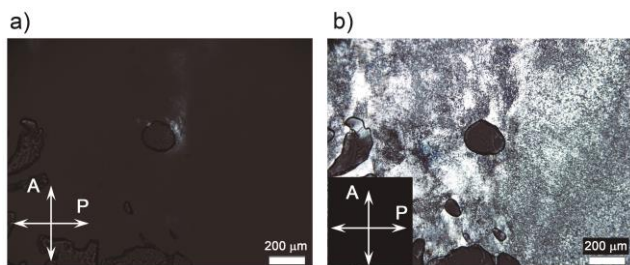


**Fig. 5** Polarizing optical microscope (POM) images of **1/Li<sup>+</sup>(50)** at a) 58 °C and b) 90 °C. A: analyzer; P: polarizer.

Compounds **1**, **2** and the mixtures **1/Li<sup>+</sup>(20)**, **1/Li<sup>+</sup>(50)**, **2/Li<sup>+</sup>(20)** and **2/Li<sup>+</sup>(50)** were selected to study the effects of addition of **PC**. Compounds **1** and **2** show biphasic behavior after addition of 5 and 10 wt% of **PC**.<sup>‡</sup> In contrast, the mixtures **1/Li<sup>+</sup>(x)** and **2/Li<sup>+</sup>(x)** form homogenous LC mixtures upon the addition of 5 or 10 wt% of **PC** [**1/Li<sup>+</sup>(x)PC(y)** and **2/Li<sup>+</sup>(x)PC(y)**, y indicates the wt% of **PC**] (Table 1).<sup>§</sup> These results suggest that **LiTFSI** is essential for the stabilization of the LC phases in the mixtures containing zwitterions **1** or **2** and **PC**. The mixtures of **2/Li<sup>+</sup>(x)PC(y)** show only  $\text{Col}_h$  phases, but the mixtures based on **1/Li<sup>+</sup>(x)PC(y)** exhibit  $\text{Cub}_{bi}$  LC phases (Table 1). This behavior also indicates that the interactions of dicyanoethenolate anion, lithium ion and **PC** play key roles in the induction of cubic phases. For example, **1/Li<sup>+</sup>(20)** shows only a  $\text{Col}_h$  phase, but  $\text{Cub}_{bi}$  phases are formed after addition of 5 or 10 wt% of **PC** (Table 1). Moreover, the cubic phase observed for **1/Li<sup>+</sup>(50)** is

thermally stabilized up to 80 °C by adding **PC** (Table 1). Remarkably, as far as we know the use of **PC** for the induction or stabilization of  $\text{Cub}_{bi}$  phases has not yet been reported.

In order to know more details about the structural organization of these complexes, we studied the XRD parameters of the LC phases of **1**, **2**, and the selected mixtures with **LiTFSI** and **LiTFSI/PC**. Table 2 displays the unit cell distances for the  $\text{Cub}_{bi}$  phases and the intercolumnar distances for the  $\text{Col}_h$  phases of the selected mixtures. Compounds **1** and **2** in the  $\text{Col}_h$  phases show intercolumnar distances of 40 Å. The molecular lengths of **1** and **2** in the extended conformation are estimated to be 33 and 30 Å, respectively. Thus, these results suggest that these zwitterionic molecules self-assemble into well-packed  $\text{Col}_h$  structures, where aliphatic chains and zwitterionic moieties are interdigitated (Fig. 1 and Fig. S9).<sup>51-54,60,63-64</sup> The addition of 50 mol% of **LiTFSI** to **1** and **2** produces an increase in the intercolumnar distances (Table 2). In the case of **2/Li<sup>+</sup>(50)**, the intercolumnar distance also increases upon the addition of 10 wt% of **PC**. Similar swelling is observed in the  $\text{Cub}_{bi}$  phases of **1/Li<sup>+</sup>(50)** after the addition of 10 wt% of **PC**, where the unit cell distance increases 2.6 Å (Table 2). These results imply that the **LiTFSI** and **PC** are incorporated within the ionic channels by interacting with the zwitterionic moieties (Fig. 1, Fig. S8, Fig. S9 and Fig. S11).

**Table 2** Lattice parameters of the LC phases determined by XRD measurements

Sample	Lattice parameters (Å)	LC phase <sup>a</sup>	Temperature (°C)
<b>1</b>	40.8	$\text{Col}_h$	120
<b>1/Li<sup>+</sup>(50)</b>	43.4	$\text{Col}_h$	120
<b>1/Li<sup>+</sup>(50)</b>	96.1	$\text{Cub}_{bi}$	55
<b>1/Li<sup>+</sup>(50)PC(10)</b>	98.7	$\text{Cub}_{bi}$	60
<b>2</b>	40.4	$\text{Col}_h$	100
<b>2/Li<sup>+</sup>(50)</b>	41.3	$\text{Col}_h$	100
<b>2/Li<sup>+</sup>(50)PC(10)</b>	42.2	$\text{Col}_h$	100

<sup>a</sup>  $\text{Col}_h$ : columnar hexagonal;  $\text{Cub}_{bi}$ : bicontinuous cubic.

### Ionic conductivities

The ionic conductivities of the zwitterions **1** and **2**, and the mixtures  $1/\text{Li}^+(\text{x})$ ,  $2/\text{Li}^+(\text{x})$ ,  $1/\text{Li}^+(\text{x})\text{PC}(\text{y})$  and  $2/\text{Li}^+(\text{x})\text{PC}(\text{y})$  were measured as a function of temperature (Fig. 6, Fig. 7 and Fig. S12) by the alternating current impedance method.<sup>33</sup> All the conductivities were measured on heating processes. Fig. 6 shows the ionic conductivities of the mixtures based on **1** (Fig. 6a) and **2** (Fig. 6b) containing 0 to 50 mol% of **LiTFSI**. All samples are not aligned. The samples exhibiting the  $\text{Col}_h$  phases show polydomain textures under POM observation (Fig. 5b). The addition of **LiTFSI** to **1** and **2** significantly increase the ionic conductivities. This observation suggests that the presence of mobile species enhances the ionic conductivities in the systems. The ionic conductivities for  $1/\text{Li}^+(\text{x})$  and  $2/\text{Li}^+(\text{x})$  increase with increasing amount of **LiTFSI**. This enhancement is more significant for the  $2/\text{Li}^+(\text{x})$  mixtures than that for the  $1/\text{Li}^+(\text{x})$  mixtures. For example, the value of the ionic conductivity of **2** at 100 °C is  $5 \times 10^{-9} \text{ S cm}^{-1}$  while  $2/\text{Li}^+(\text{50})$  mixture shows the value of  $6 \times 10^{-6} \text{ S cm}^{-1}$ . On the other hand, the addition of 50 mol% of **LiTFSI** to **1** increases the conductivity from  $1 \times 10^{-8} \text{ S cm}^{-1}$  to  $4 \times 10^{-6} \text{ S cm}^{-1}$  at 100 °C. All the mixtures show a gradual increase in the ionic conductivity with the increase of temperature. Compound  $1/\text{Li}^+(\text{50})$  shows a change in the increasing trend of the ionic conductivities between 65 and 80 °C on heating (Fig. 6a), probably due to the slow  $\text{Cub}_{\text{bi}}\text{-Col}_h$  phase transition.<sup>34,52</sup>

It is noteworthy that the highest conductivities in the  $1/\text{Li}^+(\text{x})$  and  $2/\text{Li}^+(\text{x})$  series are obtained in the 1:1 mixtures (Fig. 6). Previous works on LC lithium ion transport materials used lower amounts of lithium salts.<sup>31,55,63,64</sup> Generally, low lithium ion concentration in the electrolytes gives better ionic conductivities.<sup>67,68</sup> For example, McFarlane and coworkers reported that for the binary mixtures of *N*-alkylmethylpyrrolidinium TFSI and **LiTFSI** the conductivity continued to increase by doping less than 30 mol% of **LiTFSI** and further doping up to 50 mol% of **LiTFSI** resulted in the decrease in the conductivity.<sup>68</sup> It is assumed that in the present system the 1:1 mixtures form ionic liquid-like structures<sup>62</sup> within the ionic channels, resulting in the increase of the ionic mobility.

Interestingly, the addition of **PC** to  $1/\text{Li}^+(\text{x})$  and  $2/\text{Li}^+(\text{x})$  leads to the enhancement of ionic conductivities (Fig. 7 and Fig. S12). The ionic conductivity of  $1/\text{Li}^+(\text{50})$  increases four times after the addition of 5 or 10 wt% of **PC** (Fig. 7a). On the other hand, the stepwise increase in conductivities for  $2/\text{Li}^+(\text{50})$  is seen by adding 5 and 10 wt% of **PC** (Fig. 7b). The highest ionic conductivities in the series are observed for  $2/\text{Li}^+(\text{50})\text{PC}(\text{10})$ . The value reaches  $10^{-4} \text{ S cm}^{-1}$  at around 100 °C.<sup>†</sup>

The activation energies ( $E_a$ ) of the ion conduction were estimated for  $1/\text{Li}^+(\text{50})$  and  $1/\text{Li}^+(\text{50})\text{PC}(\text{10})$  in the  $\text{Cub}_{\text{bi}}$  phases and for  $2/\text{Li}^+(\text{50})$  and  $2/\text{Li}^+(\text{50})\text{PC}(\text{10})$  in the  $\text{Col}_h$  phases (ESI<sup>†</sup>). It was found that the  $E_a$  significantly decreased after the addition of **PC** to  $1/\text{Li}^+(\text{x})$  and  $2/\text{Li}^+(\text{x})$ . For example, the value of  $E_a$  of  $1/\text{Li}^+(\text{50})$  in the  $\text{Cub}_{\text{bi}}$  phase was  $64 \text{ kJ mol}^{-1}$ , while that for  $1/\text{Li}^+(\text{50})\text{PC}(\text{10})$  was  $41 \text{ kJ mol}^{-1}$ . In the case of  $2/\text{Li}^+(\text{50})$  and  $2/\text{Li}^+(\text{50})\text{PC}(\text{10})$  in the  $\text{Col}_h$  phase, the values are  $38 \text{ kJ mol}^{-1}$  and  $23 \text{ kJ mol}^{-1}$ , respectively. These reductions in the  $E_a$  by the addition of **PC** were attributed to the weakening of the interactions between zwitterions and lithium ion upon the formation of ion-dipole interactions among the **PC** (Fig. 3). The formation of more mobile ionic channels would facilitate the transport of lithium ions.

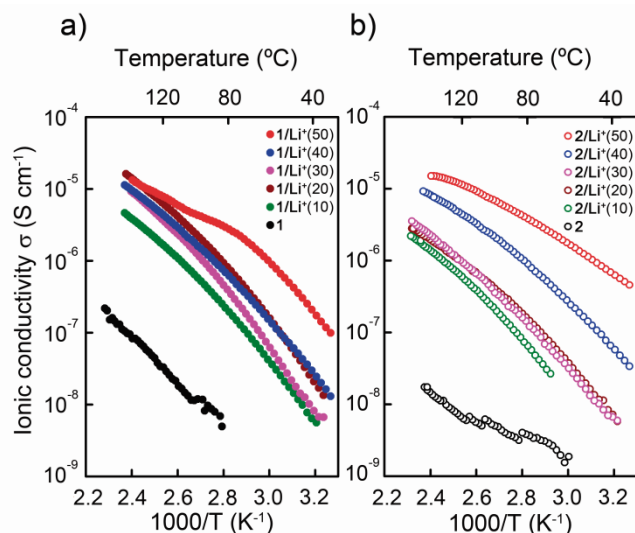


Fig. 6 Ionic conductivities as a function of temperature of a) **1** and the mixtures  $1/\text{Li}^+(\text{x})$  and b) **2** and the mixtures  $2/\text{Li}^+(\text{x})$ . x indicates the mol% of **LiTFSI**.

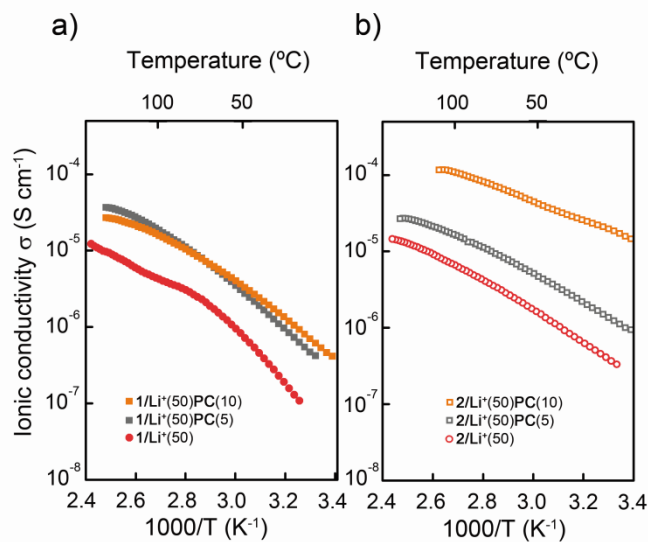


Fig. 7 Ionic conductivities as a function of temperature for the mixtures; a)  $1/\text{Li}^+(\text{50})\text{PC}(\text{y})$  and b)  $2/\text{Li}^+(\text{50})\text{PC}(\text{y})$ . y denotes the wt% of **PC**.

### Conclusions

We successfully developed 1D and 3D lithium ion transport LC materials by the co-assembly of a wedge-shaped zwitterion (**1** or **2**), **LiTFSI** and **PC**. LC zwitterions provide stable nanostructured media for the lithium ion transport and exhibit LC phases with up to 50 mol% of **LiTFSI** and up to 10 wt% of **PC**. The LC phases and ionic conductivities are tuned by the appropriate molecular design and changing the ratio of **LiTFSI** and **PC**. Remarkably, the supramolecular interactions between zwitterions, **LiTFSI** and **PC** are the key for the stabilization of LC phases and for the enhancement of conductivities. It is expected that the ionic conductivities may be further enhanced by increasing the **PC** fraction of the electrolyte materials. The system described here introduces important advances in the development of nanostructured lithium ion-conductive materials, and open new pathways for the

development of LC electrolytes that can be applied in energy devices.

## Experimental

Synthesis and characterization of compounds **1** and **2** are described in the Electronic Supporting Information (ESI†)

### Preparation of the mixtures

Compounds **1** and **2** were dried under vacuum at 80 °C for 12 h before their use. They showed no hygroscopic behavior in a period of days at ambient conditions. All the materials and solvents for the preparation of the mixtures were dried before use.

Mixtures **1**/Li<sup>+</sup>(x) and **2**/Li<sup>+</sup>(x) were prepared by adding the appropriate volume of a THF solution of LiTFSI (0.026 M) to a weighted amount of zwitterion **1** and **2** (10–30 mg) in a microtube. The solution was homogenised by sonication and then the solvent was slowly removed by rotatory evaporation. The samples were dried under vacuum at 80 °C for 12 h before their study. The presence of no volatiles was confirmed by thermogravimetric analyses (Fig. S1).

The mixtures **1**/Li<sup>+</sup>(x)PC(y) and **2**/Li<sup>+</sup>(x)PC(y) were prepared by adding the appropriate amount of PC to **1**/Li<sup>+</sup>(x) and **2**/Li<sup>+</sup>(x) respectively. The solid blend was homogenised by using a spatula and then heated to 50 °C for 5 min. These mixtures were prepared at ambient conditions in the laboratory (Humidity: 40–60 %). The presence of volatiles was monitored by thermogravimetric analyses (Fig. S1). The thermograms indicate no inclusion of volatile in the sample, but the loss of less than 1 wt% of the added PC during the sample preparation (Fig. S1).

### Acknowledgements

This study was partially supported by the Funding Program for World-Leading Innovative R&D on Science and Technology (FIRST) from the Cabinet Office, Government of Japan. This work was also partially supported by a Grant-in-Aid for Scientific Research (No. 22107003) in the Innovative Area of “Fusion Materials” (Area No. 2206) from the Ministry of Education, Culture, Sports, Science and Technology (MEXT). M. Y. is grateful for financial supports from Grant-in-Aid for Young Scientists (A) (No. 2570813) from the Japan Society for the Promotion of Science and The Noguchi Institute.

### Notes and references

<sup>a</sup> Department of Chemistry and Biotechnology, School of Engineering, The University of Tokyo, Hongo, Bunkyo-ku, Tokyo 113-8656, Japan.

<sup>b</sup> CREST, JST, 4-1-8, Honcho, Kawaguchi, Saitama, 332-0012, Japan.

<sup>c</sup> Department of Biotechnology, Tokyo University of Agriculture and Technology, Nakacho, Koganei, Tokyo 184-8588, Japan.

† Mixtures containing more than 50 mol% of LiTFSI show no homogeneous LC phases.

‡ The wt% of PC is given to the respect to the mass of zwitterion. 5 and 10 wt% of PC is roughly equivalent to 22 and 45 mol% of PC to the respect of zwitterion.

§ Mixtures **1**/Li<sup>+</sup>(x) and **2**/Li<sup>+</sup>(x) show biphasic behaviour after addition of 15 wt% or more of PC. Microscope images of a mixture exhibiting biphasic behavior are shown in Fig. S2.

¶ Thermogravimetric analyses of PC-containing mixtures indicate that the evaporation of PC under N<sub>2</sub> flow starts below 100 °C. (Fig. S1). This evaporation is lower when the samples are sandwiched.

Electronic Supplementary Information (ESI) available: [Materials and methods, synthetic procedures, characterization of compounds, thermogravimetric analyses of the materials, liquid crystalline characterization experiments including XRD patterns and POM images, <sup>7</sup>Li NMR studies, IR spectra and supplementary ion conduction measurements. See DOI: 10.1039/b000000x/

- 1 *Handbook of Liquid Crystals 2nd Ed.*, ed. J. W. Goodby, P. J. Collings, T. Kato, C. Tschierske, H. Gleeson and P. Raynes, Wiley-VCH, Weinheim, Germany, 2014.
- 2 T. Kato, N. Mizoshita and K. Kishimoto, *Angew. Chem. Int. Ed.*, 2006, **45**, 38–68.
- 3 D. J. Broer, C. M. W. Bastiaansen, M. G. Debije and A. P. H. J. Schenning, *Angew. Chem., Int. Ed.*, 2012, **51**, 7102–7109.
- 4 W. Pisula, X. Feng and K. Müllen, *Adv. Mater.*, 2010, **22**, 3634–3649.
- 5 N. Houbenov, J. S. Haataja, H. Iatrou, N. Hadjichristidis, J. Ruokolainen, C. F. J. Faul and O. Ikkala, *Angew. Chem. Int. Ed.*, 2011, **50**, 2516–2520
- 6 B. M. Rosen, C. J. Wilson, D. A. Wilson, M. Peterca, M. R. Imam and V. Percec, *Chem. Rev.*, 2009, **109**, 6275–6540.
- 7 T. Kato, *Science*, 2002, **295**, 2414–2418.
- 8 S. Chen, S. H. Eichhorn, *Isr. J. Chem.*, 2012, **52**, 830–843.
- 9 C. F. J. Faul and M. Antonietti, *Adv. Mater.*, 2003, **15**, 673–683.
- 10 B. R. Wiesenauer and D. L. Gin, *Polym. J.*, 2012, **44**, 461–468.
- 11 D. L. Gin, C. S. Pecinovsky, J. E. Bara and R. L. Kerr, *Struct. Bonding*, 2008, **128**, 181–222.
- 12 M. Funahashi, H. Shimura, M. Yoshio and T. Kato, *Struct. Bonding*, 2008, **128**, 151–180.
- 13 S. Sergeyev, W. Pisula and Y. H. Geerts, *Chem. Soc. Rev.*, 2007, **36**, 1902–1929.
- 14 K. Binnemans, *Chem. Rev.*, 2005, **105**, 4148–4204.
- 15 T. Kato, *Angew. Chem. Int. Ed.*, 2010, **49**, 7847–7848.
- 16 I. M. Saez, and R. J. W. Goodby, *Struct. Bonding*, 2008, **128**, 1–62.
- 17 C. Tschierske, *Chem. Soc. Rev.*, 2007, **36**, 1930–1970.
- 18 B. Donnio, S. Buathong, I. Bury and D. Guillon, *Chem. Soc. Rev.*, 2007, **36**, 1495–1513.
- 19 M. Marcos, R. Martín-Rapún, A. Omenat and J. L. Serrano, *Chem. Soc. Rev.*, 2007, **36**, 1889–1901.
- 20 M. Yoshio and T. Kato, in *Handbook of Liquid Crystals 2nd Ed.*; ed. J. W. Goodby, P. J. Collings, T. Kato, C. Tschierske, H. Gleeson and P. Raynes; Wiley-VCH, Weinheim, 2014, vol. 8, ch. 23, pp 727–749.
- 21 C. F. vanNostrum and R. J. M. Nolte, *Chem. Commun.*, 1996, 2385–2392.
- 22 Y. G. Zheng, J. G. Liu, Y. P. Liao, G. Ungar and P. V. Wright, *Dalton Trans.*, 2004, 3053–3060.
- 23 U. Beginn, G. Zipp and M. Moller, *Adv. Mater.*, 2000, **12**, 510–511.
- 24 N. Sakai and S. Matile, *Langmuir*, 2013, **29**, 9031–9040.
- 25 M. Armand and J. M. Tarascon, *Nature*, 2008, **451**, 652–657.
- 26 Y. B. Chen, M. Thorn, S. Christensen, C. Versek, A. Poe, R. C. Hayward, M. T. Tuominen and S. Thayumanavan, *Nat. Chem.*, 2010, **2**, 503–508.
- 27 Y. Kim, W. Li, S. Shin and M. Lee, *Acc. Chem. Res.*, 2013, **46**, 2888–2897.

- 28 B.-K. Cho, A. Jain, S. M. Gruner and U. Wiesner, *Science*, 2004, **305**, 1598–1601.
- 29 H.-K. Lee, H. Lee, Y. H. Ko, Y. J. Chang, N.-K. Oh, W.-C. Zin and K. Kim, *Angew. Chem., Int. Ed.*, 2001, **40**, 2669–2671.
- 30 V. Percec, G. Johansson, J. Heck, G. Ungar and S. V. Batty, *J. Chem. Soc., Perkin Trans. 1*, 1993, 1411–1420.
- 31 R. L. Kerr, S. A. Miller, R. K. Shoemaker, B. J. Elliott and D. L. Gin, *J. Am. Chem. Soc.*, 2009, **131**, 15972–15972.
- 32 M. Yoshio, T. Mukai, K. Kanie, M. Yoshizawa, H. Ohno and T. Kato, *Adv. Mater.*, 2002, **14**, 351–354.
- 33 M. Yoshio, T. Mukai, H. Ohno and T. Kato, *J. Am. Chem. Soc.*, 2004, **126**, 994–995.
- 34 T. Ichikawa, M. Yoshio, A. Hamasaki, T. Mukai, H. Ohno and T. Kato, *J. Am. Chem. Soc.*, 2007, **129**, 10662–10663.
- 35 M. Yoshio, T. Ichikawa, H. Shimura, T. Kagata, A. Hamasaki, T. Mukai, H. Ohno and T. Kato, *Bull. Chem. Soc. Jpn.*, 2007, **80**, 1836–1841.
- 36 T. Ohtake, M. Ogasawara, K. Ito-Akita, N. Nishina, S. Ujiie, H. Ohno and T. Kato, *Chem. Mater.*, 2000, **12**, 782–789.
- 37 P. H. J. Kouwer and T. M. Swager, *J. Am. Chem. Soc.*, 2007, **129**, 14042–14052.
- 38 B.-K. Cho, *RSC Advances*, 2014, **4**, 395–405.
- 39 K. Kishimoto, M. Yoshio, T. Mukai, M. Yoshizawa, H. Ohno and T. Kato, *J. Am. Chem. Soc.*, 2003, **125**, 3196–3197.
- 40 H. Shimura, M. Yoshio, A. Hamasaki, T. Mukai, H. Ohno and T. Kato, *Adv. Mater.*, 2009, **21**, 1591–1594.
- 41 X. Feng, M. E. Tousley, M. G. Cowan, B. R. Wiesenauer, S. Nejati, Y. Choo, R. D. Noble, M. Elimelech, D. L. Gin and C. O. Osuji, *ACS Nano*, 2014, **8**, 11977–11986.
- 42 B. Soberats, E. Uchida, M. Yoshio, J. Kagimoto, H. Ohno and T. Kato, *J. Am. Chem. Soc.*, 2014, **136**, 9552–9555.
- 43 A. Yamashita, M. Yoshio, S. Shimizu, T. Ichikawa, H. Ohno and T. Kato, *J. Polym. Sci. Part A: Polym. Chem.*, 2014, DOI: 10.1002/pola.27380.
- 44 T. Ichikawa, M. Yoshio, A. Hamasaki, S. Taguchi, F. Liu, X. B. Zeng, G. Ungar, H. Ohno and T. Kato, *J. Am. Chem. Soc.*, 2012, **134**, 2634–2643.
- 45 S. Kutsumizu, *Isr. J. Chem.*, 2012, **52**, 844–853.
- 46 E. S. Hatakeyama, B. R. Wiesenauer, C. J. Gabriel, R. D. Noble and D. L. Gin, *Chem. Mater.*, 2010, **22**, 4525–4527.
- 47 D. Högberg, B. Soberats, S. Uchida, L. Kloo, H. Segawa and T. Kato, *Chem. Mater.*, 2014, **26**, 6496–6502.
- 48 J. Sakuda, E. Hosono, M. Yoshio, T. Ichikawa, T. Matsumoto, H. Ohno, H. Zhou and T. Kato, *Adv. Funct. Mater.*, 2014, DOI: 10.1002/adfm.201402509
- 49 R. D. Costa, F. Werner, X. J. Wang, P. Groninger, S. Feihl, F. T. U. Kohler, P. Wasserscheid, S. Hibler, R. Beranek, K. Meyer and D. M. Guldi, *Adv. Energy Mater.*, 2013, **3**, 657–665.
- 50 N. Yamanaka, R. Kawano, W. Kubo, N. Masaki, T. Kitamura, Y. Wada, M. Watanabe and S. Yanagida, *J. Phys. Chem. B*, 2007, **111**, 4763–4769.
- 51 T. Ichikawa, M. Yoshio, S. Taguchi, J. Kagimoto, H. Ohno and T. Kato, *Chem. Sci.* 2012, **3**, 2001–2008.
- 52 B. Soberats, M. Yoshio, T. Ichikawa, S. Taguchi, H. Ohno and T. Kato, *J. Am. Chem. Soc.*, 2013, **135**, 15286–15289.
- 53 T. Ichikawa, T. Kato and H. Ohno, *J. Am. Chem. Soc.*, 2012, **134**, 11354–11357.
- 54 T. Matsumoto, T. Ichikawa, J. Sakuda, T. Kato and H. Ohno, *Bull. Chem. Soc. Jpn.*, 2014, **87**, 792–796.
- 55 T. Ichikawa, M. Yoshio, A. Hamasaki, J. Kagimoto, H. Ohno and T. Kato, *J. Am. Chem. Soc.*, 2011, **133**, 2163–2169.
- 56 W. J. Middleton and V. A. Engelhardt, *J. Am. Chem. Soc.*, 1958, **80**, 2788–2794.
- 57 M.-L. Pujol-Fortin and J.-C. Galin, *Macromolecules*, 1991, **24**, 4523–4530.
- 58 M. Galin, A. Chapoton and J. C. Galin, *J. Chem. Soc. Perkin Trans. 2*, 1993, 545–553.
- 59 A. Mathis, M. Galin, J. C. Galin, B. Heinrich and C. G. Bazuin, *Liq. Cryst.*, 1999, **26**, 973–984.
- 60 S. Ueda, J. Kagimoto, T. Ichikawa, T. Kato and H. Ohno, *Adv. Mater.*, 2011, **23**, 3071–3074.
- 61 K. Xu, *Chem. Rev.*, 2004, **104**, 4303–4417.
- 62 M. Yoshizawa, A. Narita and H. Ohno, *Aust. J. Chem.*, 2004, **57**, 139–144.
- 63 J. C. Y. Lin, C.-J. Huang, Y.-T. Lee, K.-M. Lee and I. J. B. Lin, *J. Mater. Chem.*, 2011, **21**, 8110–8121.
- 64 R. Rondla, J. C. Y. Lin, C. T. Yang and I. J. B. Lin, *Langmuir*, 2013, **29**, 11779–11785.
- 65 M. Yoshizawa, M. Hirao, K. Ito-Akita and H. Ohno, *J. Mater. Chem.*, 2001, **11**, 1057–1062.
- 66 H. Lee, D. B. Kim, S.-H. Kim, H. S. Kim, S. J. Kim, D. K. Choi, Y. S. Kang and J. Won, *Angew. Chem. Int. Ed.*, 2004, **43**, 3053–3056.
- 67 S. Sylla, J.-Y. Sanchez and M. Armand, *Electrochim. Acta*, 1992, **37**, 1699–1701.
- 68 D. R. MacFarlane, J. Huang and M. Forsyth, *Nature*, 1999, **402**, 792–794.